A&A 455, 131–134 (2006)
DOI: 10.1051/0004-6361:20054219

Astronomy & Astrophysics

3D spectroscopy with VLT/GIRAFFE

III. Mapping electron densities in distant galaxies⋆

M. Puech[1], H. Flores[1], F. Hammer[1], and M. D. Lehnert[2]

[1] Laboratoire Galaxies Etoiles Physique et Instrumentation, Observatoire de Paris, 5 place Jules Janssen, 92195 Meudon, France
e-mail: mathieu.puech@obspm.fr
[2] Max-Planck-Institut für extraterrestrische Physik, Giessenbachstrasse, 85748 Garching bei München, Germany

Received 16 September 2005 / Accepted 17 January 2006

ABSTRACT

We used the moderately high spectral resolution of FLAMES/GIRAFFE (R = 10 000) to derive electron densities from [OII] line ratios in 6 galaxies at $z \sim 0.55$. These measurements have been done through the GIRAFFE multiple integral field units and are the very first *mapping* of electron densities in such distant objects. This allows us to confirm an outflow and identify the role of giant HII regions in galactic disks. Such measurements could be used in the future to investigate the nature of the physical processes responsible for the high star formations rates observed in galaxies between $z \sim 0.4$ and $z \sim 1$.

Key words. galaxies: kinematics and dynamics – galaxies: ISM

1. Introduction

It is now well established that the cosmic star formation density declines from $z \sim 1$ to 0 (Lilly et al. 1996; Madau et al. 1998; Flores et al. 1999; Le Floc'h et al. 2005). However, the physical processes responsible for this decline are still a matter of debate. At the heart of this debate is the respective importance of secular evolution with slow and continuous external matter accretion (e.g. Semelin & Combes 2005) versus more violent evolution through hierarchical merging (e.g. Hammer et al. 2005) as a function of lookback time. Relating star formation processes with the ISM state (i.e. its chemistry *and* kinematics) of distant galaxies could provide a new insight into this debate. We present in this paper the first mapping of electron density in a small sample of distant galaxies. Our goal is to demonstrate the feasibility of such measurements using current integral field spectrographs on a 8 meter telescope. In the future, we will investigate the possible relations between such quantities (e.g. electron density, metal abundance ...) and the star formation rate. Their possible correlations could help in constraining the physical processes at work in galaxies, those which are responsible for the strong evolution of the cosmic star formation density.

Electron density can be determined from the intensity ratio of two lines of the same ion arising from levels with nearly the same excitation energy (Osterbrock & Ferland 2006). The lines usually used are the [OII]$\lambda\lambda$3729, 3726 Å and the [SII]$\lambda\lambda$6716, 6731 Å doublets. For distant galaxies, the [OII] doublet becomes particularly well suited to probe electron densities, although local [OII] variations in galaxies are more sensitive to extinction and metallicity (e.g. Kewley et al. 2004; Mouhcine et al. 2005). First determination of electron density N_e from [OII]$\lambda\lambda$3727, 3729 Å line ratio $r = 3729/3727$ in nebulae has been suggested by Aller et al. (1949). The relation between r, N_e and electron temperature T_e has been successively improved by Seaton et al. (1954) and Eissner et al. (1969). First confrontations with observations were done in several nearby nebulae with good agreement (Seaton & Osterbrock 1957). Because r only depends weakly on T_e (see e.g. Canto et al. 1980), this relation provides a good mean to measure N_e and then investigate the structure of HII regions such as Orion (Osterbrock et al. 1959; Danks et al. 1971; Canto et al. 1980) or M 8 (Meaburn et al. 1969), and of planetary nebulae (see Osterbrock & Ferland 2006, and references therein). More recent studies of several HII regions have been carried out by Copetti et al. (2000) in our Galaxy and by Castaneda et al. (1992) in the local group.

We recently used the FLAMES/GIRAFFE spectrograph at ESO/VLT in its multi-IFU mode to target the [OII] doublet of 35 galaxies at $z \sim 0.55$ in order to obtain their kinematics (see Paper I, Flores et al. 2006; and Paper II, Puech et al. 2006). Thanks to the excellent spectral resolution of GIRAFFE ($R \sim$ 10 000), we have used here a part of this sample to derive the electron density maps of a few distant galaxies. This paper is organized as follows: Sect. 2 presents the sample and the methodology, results are in Sect. 3 and Sect. 4 gives a conclusion.

2. Sample, observations and methodology

As part of the GTO of the Paris Observatory, we obtained FLAMES/GIRAFFE-IFU (3 by 2 arcsec^2, 0.52 arcsec/pixel) observations for 35 galaxies at $0.4 \leq z \leq 0.71$ in the CFRS (03 h and 22 h) and HDFS field. The complete sample is described in Paper I (Flores et al. 2006) and the Luminous Compact Galaxies (LCGs) sub-sample in Paper II (Puech et al. 2006). Briefly, we used LR04 and LR05 setups targeting the [OII] doublet ($R \sim$ 10 000) with integration times ranging from 8 to 13 h. Seeing was typically ∼0.6 arcsec during all the observations. Datacubes were reduced using the GIRBLDRS v1.12 package (Blecha et al. 2000), including narrow flat-fielding, and the sky was carefully subtracted using our own IDL procedures.

Among these 35 galaxies, we selected those for which at least 1.5 spatial resolution element had [OII] doublets reaching

⋆ Based on observations collected at the European Southern Observatory, Paranal, Chile, ESO Nos 71.A-0322(A) and 72.A-0169(A).

Table 1. Main properties of the sample of galaxies: galaxy names, redshifts, isophotal I magnitude and absolute B magnitude (from Hammer et al. 2005).

ID	z	I_{AB}	M_B
CFRS03.0488	0.6069	21.58	−20.37
CFRS03.0508	0.4642	21.92	−19.61
CFRS03.0645	0.5275	21.36	−20.30
CFRS03.9003	0.6189	20.77	−21.24
CFRS22.0504	0.5379	21.02	−20.52
CFRS22.0919	0.4738	21.77	−19.99

a mean *SNR* per resolution element of 8 (see Paper I). This allows the establishment of meaningful electron density maps, i.e. with at least 6 pixel among the 20 composing the GIRAFFE IFU. For galaxies with complex kinematics, the large pixel size of GIRAFFE integrates both random motions and larger scale motions. This tends to blend the [OII] doublet in these kinds of galaxies in spite of the high spectral resolution of GIRAFFE (∼10 000, see Paper I, Flores et al. 2006). For the present study, we discarded all galaxies where this effect could lead to a too high uncertainty on the [OII] line ratio measurement. We finally selected 6 galaxies (see Table 1) among those having the highest quality factor of the whole sample (Paper I, Flores et al. 2006).

[OII] doublets were fitted after a slight Savitzky-Golay filtering which has the advantage of conserving the first moments of the spectral lines (Press et al. 1989). During the fit we used the following constraints: $\lambda_2 - \lambda_1 = 2.783$ Å and $\sigma_1 = \sigma_2$ (see Paper I, Flores et al. 2006; and Paper II, Puech et al. 2006, for the detailed procedure). We checked by visual inspection each fit and discarded a total of 4 pixel (≤1% of pixel) where the results were particularly uncertain, mostly due to noisy peaks or extinction effects. We then derived [OII] distribution maps by simply integrating the fitted doublets in each pixel. [OII] line ratio was related to electron density using n-levels atom calculations of the stsdas/Temden IRAF task. The relation linking r, N_e and T_e depends only weakly on T_e in the range of temperatures of the regions studied (see Eissner et al. 1969; Canto et al. 1980): we took $T_e = 10\,000$ K in all the sample, which is a good approximation for most of HII regions (Osterbrock & Ferland 2006). The maximal value of the line ratio r in this calibration is then 1.492. Using some different collision strengths from Mendoza (1983), one can derive a maximal ratio of 1.497 (J. Walsh, private communication). Given our uncertainty on the measurement of r (0.05, see below), one can derive an upper limit of 1.56 for acceptable measures of r: we checked that all the measured line ratio were lower than this limit, and forced all line ratio greater than 1.492 (and lower than 1.56) to 1.492 (the last point in the calibration). This corresponds to a density of ∼1 cm^{-3} and affects ∼8% of the pixels.

The main sources of errors in the determination of electron density are twofold. The first one is the error on the determination of r during the fit: compared to line positions and widths, [OII] line ratios are the less well determined parameters of the fit because it is more sensitive to noise. We estimated this error to be typically ∼0.05 (3σ) on r. For example, for a ratio $r = 1.3$, one derives $N = 101^{+33}_{-29}$ cm^{-3}. The second one is due to the saturation of the r vs. N_e relation at low densities (typically at $N_e \lesssim 10$ cm^{-3}) and is very difficult to estimate. As already mentioned above, we tried to minimize these effects by limiting the measurement of r to the highest *SNR* pixels reaching a mean *SNR* per spectral resolution element greater than 8 which corresponds to a higher threshold than the one used for the other maps (see Paper I, Flores et al. 2006). Finally, the main uncertainty results from extinction effects: as the [OII] emission line can be severely affected by extinction (see e.g. Hammer et al. 2005), some local density peaks could be hidden by dust and then undetected by the [OII] line ratio diagnostic.

Finally, given the GIRAFFE IFU spatial resolution (20 pixel), we interpolated all maps (velocity fields, σ-maps, electron density maps and [OII] fluxes maps) by a simple 5×5 linear interpolation to make visualization easier (see Fig. 1).

3. Results

CFRS03.0488. This galaxy has an asymmetric morphology which is usually believed to be a signature of interactions and/or gas accretion. Its kinematics is classified as complex by Paper I (Flores et al. 2006). The [OII] map shows a peak off centered relative to the brighter component of the galaxy, i.e. in the diffuse component (above the main optical component), apparently correlated with a higher electron density region. Densities are in the range [30–153] cm^{-3} which are typical of classical HII regions (Copetti et al. 2000). The higher densities observed in the diffuse component could be explained by collisions between molecular clouds of the interstellar medium and gas inflow/outflow events, which are suggested by the morphology.

CFRS03.0508. This Luminous Compact Galaxy (LCG) was classified by Zheng et al. (2005) as a relic of an interaction or fusion, with a relatively blue color over the whole galaxy which is also seen in the [OII] map. In Paper II (Puech et al. 2006), we found that its kinematics show a rotational motion pattern with an axis almost perpendicular to the main optical axis of the galaxy, which probably reflects an outflow motion rather than a rotational motion. Electron densities are characteristic of classical HII region (≤100 cm^{-3}), higher concentrations being well aligned along the supposed outflow (maximal densities are pointing to maximal velocities ends). We believe this supports the outflow hypothesis, because in such a case, electrons are produced from collisions between the expelled gas and molecular clouds of the interstellar medium.

CFRS03.0645. Zheng et al. (2005) found in this LCG a relatively blue color all over the galaxy and classified it as a probable merger. The [OII] map shows a peak in the central region. As for CFRS03.0508, we found in Paper II (Puech et al. 2006) a kinematics showing a rotational motion pattern with an axis almost perpendicular to the main optical axis of the galaxy, which could reflect an outflow motion rather than a rotational motion. The σ-map has a peak at the edge of the galaxy, where the two main components join. Electron densities are characteristic of classical HII regions (∼100 cm^{-3}) and a peak at ∼200 cm^{-3} is found near the main optical component (at the upper right of the image). Unfortunately, the *SNR* was too low to map the diffuse component at the bottom of the HST image, and thus we cannot confirm the suspected outflow.

CFRS03.9003. This Luminous IR Galaxy (LIRG, $SFR \sim 75\ M_\odot$/yr, see Flores et al. 2004) presents a quite complex and irregular brightness distribution. Its kinematics is classified as a rotating disk by Paper I (Flores et al. 2006). Zheng et al. (2004) found blue star-forming regions surrounding a red central region that might be a bulge. The

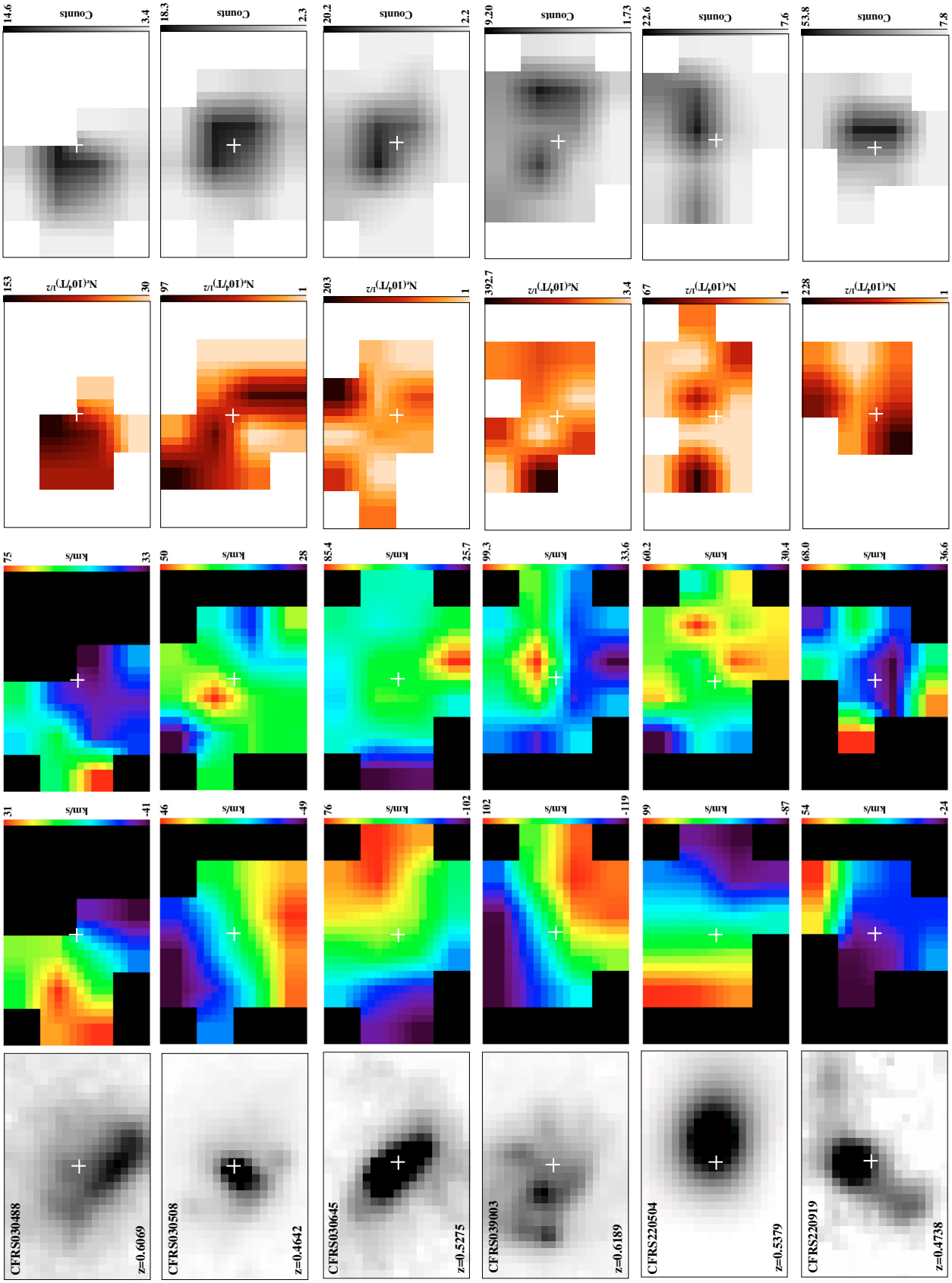

Fig. 1. Mapping of 6 distant galaxies. All maps have a scale of ~0.1 arcsec/pix and show the same FoV (3×2 arcsec^2). *From left to right*: *I* band HST imaging except CFRS220504 (deconvolved CFHT image, see text); velocity field (5×5 interpolation), σ-map (5×5 interpolation), electron density map (5×5 interpolation), and [OII] counts distribution map (5×5 interpolation). Electron density maps have been restricted in *SNR* (see text).

[OII] counts distribution is relatively flat (between ∼2 and 9) but present a small relative maximum (on the right of the image) which is located in the disk. The central region has a very low density (i.e. a few cm^{-3}) comparable with those of free electrons in the interstellar gas outside of HII regions (Reynolds 1989): this corresponds to a gas poor region and it is consistent with the presence of a bulge in this galaxy. The off centered knot in the *I* band HST image corresponds to a blue region with a peak in electron density. Paper I (Flores et al. 2006) showed that this knot is not due to a minor merger since no perturbation was seen in its kinematics (see Fig. 1). We found a significantly higher density in this region (almost 400 cm^{-3}), comparable with those found in the outer areas of some nearby nebulae, such as M 8 or Orion (Meaburn 1969; Osterbrock et al. 1959). This relatively high density could, at least partly, contribute to the very high *SFR* observed in this LIRG. The knot observed in the HST image is thus probably an extremely large HII region (∼2 kpc, a complex of several HII region?) undergoing a strong star formation episode.

CFRS22.0504. Its kinematics is classified by Paper I (Flores et al. 2006) as rotating disk. Electron densities are higher near the edges. The [OII] map shows maxima near the center and also in a region near the edge where we can also see a peak (67 cm^{-3}) in the electron density map. This probably indicates a star forming region in the disk. Unfortunately, we only had at our disposal a (deconvolved) CFHT image (0.207 arcsec/pix) to be used for comparison.

CFRS22.0919. The morphology of this LCG shows two tails on each side, characteristic of interacting systems. Its kinematics is classified complex by Paper II (Puech et al. 2006) which further supports a merger hypothesis. Electron densities peak in the tails (≥200 cm^{-3}) which corresponds to what is expected in interacting systems.

4. Discussion and conclusion

We measured [OII] doublet lines ratio of 6 galaxies with high *SNR* to derive the first mapping of electron density in $z \sim 0.6$ galaxies. The sample of the 6 objects presented here includes a large variety of objects with obvious merger (CFRS22.0919), suspected outflows (CFRS03.0508 and CFRS03.0645), and spiral galaxies (CFRS22.0504) including a LIRG (CFRS03.9003). Such a mapping can be very powerful for understanding the physical processes at work in these galaxies. The most spectacular illustrations are CFRS03.0508 where an outflow has been confirmed and CFRS03.9003 where a giant HII region has been identified. We also derive maps of [OII] total counts. For the 3 LCGs of the sample, we find that the [OII] maps show a peak at their centers, corresponding to the relatively blue cores found by Zheng et al. (2005). For the 2 rotating disks (CFRS03.9003 and CFRS22.0504), [OII] counts are distributed over the disks. This confirms that star formation migrates from center to the outskirts of the disk when comparing LCGs to spirals (Zheng et al. 2005).

The main limitation of our results arises from the fact that GIRAFFE has a relatively low spatial resolution (0.52 arcsec/pix): this makes the derived electron densities underestimated because they are averaged on spatial regions bigger than the characteristic length of HII regions (∼100 pc). Another consequence of the low spatial resolution of GIRAFFE is that line widths are the convolution of random motions with larger scale motions. In the case of merging systems where velocities can be particularly high (see Paper I, Flores et al. 2006), this makes the [OII] doublet blended in spite of the high spectral resolution of GIRAFFE ($R \sim 10\,000$) and of the *SNR* level, and then only velocities and σ can safely be recovered. Mapping such galaxies with complex kinematics are currently beyond the capabilities of an Integral Field Spectroscopy on 8 m telescopes because it would require a much higher spectral and spatial resolution. Finally, another important limitation can be due to extinction by dust which could hide some density peaks: only the unobscured regions can contributed to the [OII] flux detected, and the density maps are thus biased toward these regions.

With the arrival of Integral Field Spectrograph operating in the NIR (such as SINFONI), it is now possible to extend this kind of mapping to other physico-chemical parameters such as extinction, instantaneous *SFR* and metal abundance. The investigations of possible correlations between these quantities would probably shed a new light in the processes leading to the intense star formation rates observed at $z \geq 0.4$ and the decrease of the cosmic star formation density since $z \sim 1$.

Acknowledgements. We wish to thank ESO Paranal staff for their reception and their very useful advises during observations. We also thank A. Rawat for improving the English of this paper and the referee, Pr. J. M. Vilchez, for comments and suggestions. We thank all the team of GIRAFFE at Paris Observatory, at Geneve Observatory and at ESO for the remarkable accomplishment of this unique instrument, without which, none of these results would be obtained.

References

Aller, L. H., Ufford, C. W., & Van Vleck, J. H. 1949, ApJ, 109, 42
Blecha, A., Cayatte, V., North, P., et al. 2000, Optical and IR Telescope Instrumentation and Detectors, ed. Masanori Iye, & Alan F. Moorwood, SPIE Proc., 008, 467
Canto, J., Elliott, K. H., Meaburn, J., et al. 1980, MNRAS, 193, 911
Castaneda, H. O., Vilchez, J. M., & Copetti, M. V. F. 1992, A&A, 260, 370
Copetti, M. V. F., Mallmann, J. A. H, Schmidt, A. A., et al. 2000, A&A, 357, 621
Danks, A. C., & Meaburn, J. 1971, Ap&SS, 11, 398
Eissner, W., Martins, P. de A. P., Nussbaumer, H., et al. 1969, MNRAS, 146, 63
Flores, H., Hammer, F., Thuan, T. X., et al. 1999, ApJ, 517, 148
Flores, H., Hammer, F., Elbaz, D., et al. 2004, A&A, 415, 885
Flores, H., Hammer, F., Puech, M., et al. 2006, A&A, 455, 107 (Paper I)
Flores, H., Puech, M., Hammer, F., et al. 2004, A&A, 420, L31
Flower, D. R., & Seaton, M. J. 1969, Mém. Roy. Sci. Liège, 17, 251
Hammer, F., Flores, H., Elbaz, D., et al. 2005, A&A, 430, 115
Kewley, L. J., Geller, M. J., & Jansen, R. A. 2004, AJ, 127, 2002
Le Floc'h, E., Papovitch, C., Dole, H., et al. 2005, ApJ, accepted [arXiv:astro-ph/0506462]
Lilly, S. J., Le Fevre, O., Hammer, F., et al. 1996, ApJ, 460, 1
Madau, P., Pozzetti, L., & Dickinson, M. 1998, ApJ, 498, 106
Meaburn, J. 1969, Ap&SS, 3, 600
Mendoza, C. 1983, in Planetary Nebulae, IAU Symp., 103 (Holland, Reidel: Flower)
Mc Keith, C. D., Greve, A., Downes, D., et al. 1995, A&A, 293, 703
Mouhcine, M., Lewis, I., Jones, B., et al. 2005, MNRAS, 362, 1143
Nakamura, O., Fukugita, M., Brinkmann, J., et al. 2004, AJ, 127, 2511
Osterbrock, D., & Flather, E. 1959, ApJ, 129, 26
Osterbrock, D., & Ferland, G. 2006, Astrophysics of Gaseous Nebulae and active Galactic Nuclei, Second edition (Sausalito, California: University Science Books)
Press, W. H., Flannery, B. P., Teukolsky, S. A., et al. 1989, Numerical recipes in C (Cambridge University Press)
Puech, M., Hammer, F., Flores, H., et al. 2006, A&A, 455, 119 (Paper II)
Reynolds, R. J. 1989, ApJ, 339, L29
Schade, D., Lilly, S. J., & Crampton, D. 1995, ApJ, 451, 1
Schade, D., Lilly, S. J., & Le Fevre, O. 1996, ApJ, 464, 79
Seaton, M. J. 1954, AnAp, 17, 74
Seaton, M. J., & Osterbrock, D. E. 1957, 125, 66
Semelin, B., & Combes, F. 2005, A&A, 441, 55
Zheng, X. Z., Hammer, F., Flores, H., et al. 2004, A&A, 421, 847
Zheng, X. Z., Hammer, F., Flores, H., et al. 2005, A&A, 435, 507